

## High resolution x-ray microscope

C. K. Gary,<sup>a)</sup> H. Park,<sup>b)</sup> L. W. Lombardo, M. A. Piestrup, and J. T. Cremer  
Adelphi Technology, Inc. 981-B Industrial Road, San Carlos, California 94070

R. H. Pantell

Department of Electrical Engineering, Stanford University, Stanford, California 94305

Y. I. Dudchik

Institute of Applied Physics Problems, Kurchatova 7, Minsk 220064, Belarus

(Received 6 February 2007; accepted 4 April 2007; published online 1 May 2007)

The authors present x-ray images of grid meshes and biological material obtained using a microspot x-ray tube with a multilayer optic and a 92-element parabolic compound refractive lens (CRL) made of a plastic containing only hydrogen and carbon. Images obtained using this apparatus are compared with those using an area source with a spherical lens and a spherical lens with multilayer condenser. The authors found the best image quality using the multilayer condenser with a parabolic lens, compared to images with a spherical lens and without the multilayer optics. The resolution was measured using a 155-element parabolic CRL and a multilayer condenser with the microspot tube. The experiment demonstrates about 1.1  $\mu\text{m}$  resolution. © 2007 American Institute of Physics.  
[DOI: 10.1063/1.2734895]

We report the images taken from an x-ray microscope using a microspot x-ray tube with a multilayer optic and a parabolic compound refractive lens (CRL). The images taken with the parabolic lens microscope are compared to those taken by a bubble CRL (Ref. 1 and 2) with and without the multilayer optic.

Previously, well-aligned and closely spaced series of biconcave refractive lenses have been used in a simple microscopes for imaging using synchrotron sources.<sup>3,4</sup> Each biconcave lens has a focal length of  $f' = R/\delta$  and the series of  $N$  planoconcave unit lenses forms a CRL with a total focal length  $f_0 = f'/N$ , where the complex refractive index of the unit lens material is  $n = 1 - \delta + i(\lambda\mu/4\pi)$ ,  $\delta$  is the index decrement,  $\mu$  is the linear attenuation coefficient,  $R$  is the radius of curvature of the lens,  $t$  is the thickness of the lens, and  $\lambda$  is the x-ray wavelength.<sup>5</sup>

For a thick CRL, the focal length  $F$  is given by<sup>6</sup>

$$\frac{f}{f_0} = \frac{(tf_0)^{1/2}}{\sin(tf_0)^{1/2}}. \quad (1)$$

The parabolic CRL is composed of many biconcave parabolic lenses. We melted a plastic containing only carbon and hydrogen and molded it into lenses with Al parabolic shape masters. These low atomic-number materials were chosen for the plastic due to their better x-ray focusing ability compared to higher atomic-number elements. The Al masters were designed to have a 50  $\mu\text{m}$  radius of curvature and were micromachined. Figure 1 shows a scanning electron microscopy (SEM) photograph of an Al master. The molded polymer disks, made with the Al master, have a dimple in the center. The polymer in the dimple forms a biconcave parabolic lens. Those disks are closely stacked inside a stainless tube to form a parabolic CRL.

Such a lens can be used for magnification of an object, behaving like an ordinary optical lens in that it obeys the lens

formula,  $1/o + 1/i = 1/f$ , where  $o$  is the object distance and  $i$  is the image distance, as shown in Fig. 2. Like a simple optical microscope, the magnification is given by  $M = i/o$ .

The walls of the lenses absorb x-rays, causing the thicker edges of the biconcave lenses to limit the aperture of the CRL. This absorption aperture as a function of  $f$  is<sup>5</sup>

$$2r_a = 4 \left( \frac{\delta f}{\mu} \right)^{1/2}, \quad (2)$$

This implies that the aperture and, consequently, other important lens parameters, such as resolution and depth of field of a CRL, are determined by the required focal length and the choice of material of which the lenses are made. In the experiment two parabolic CRLs were used: a 92-element lens and a 155-element lens. The 92-element lens has a 15.3 cm focal length and the absorption aperture was 133  $\mu\text{m}$ . Thus the numerical aperture (NA) was  $4.3 \times 10^{-4}$ . The 155-element lens has a 9.3 cm focal length; the absorp-

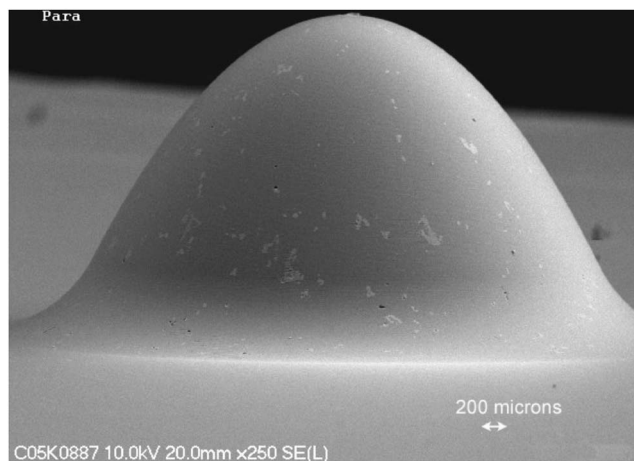


FIG. 1. SEM photograph of an Al master to mold plastic parabolic CRLs. The shape of the master is  $y = R^2/100 \mu\text{m}$ , where  $y$  is the vertical dimension and  $R$  is the horizontal dimension. The radius of curvature of the lens is 50  $\mu\text{m}$ .

<sup>a)</sup>FAX: 650-598-9400; electronic mail: cgary@adelphitech.com

<sup>b)</sup>Electronic mail: hpark@adelphitech.com

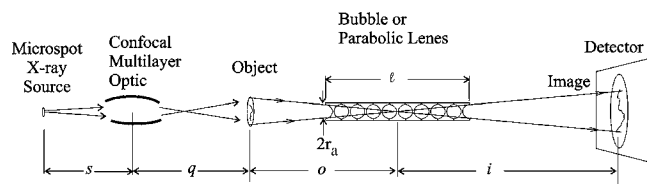


FIG. 2. X-ray microscope with a multilayer optic whose magnification is the ratio of the image  $i$  over the object distance  $o$ .

tion aperture was  $104\ \mu\text{m}$ , and the NA was  $5.6 \times 10^{-4}$ .

The microscope consists of four main components: an x-ray source (a microspot x-ray tube or an area x-ray tube), multilayer optics, a CRL (parabolic coin CRL or a spherical bubble CRL), and an x-ray detector. The positioning of the various components is shown in Fig. 2. The two x-ray sources that were used are (a) a microspot x-ray tube with a Cu anode, Apogee XTG5011 from Oxford Instruments. The nominal focal spot size is  $35\ \mu\text{m}$  and (b) a Brand X-ray Cu anode x-ray tube with an apparent source size of  $5 \times 5\ \text{mm}^2$ . The electron-tube voltage was set to 25 keV and a current of 1 mA, resulting in a standard bremsstrahlung and 8 keV characteristic-line spectra from the microspot tube with no filtering. The Brand X-ray area tube was operated at 30 kV and 15 mA. The detector consists of a Peltier-cooled, 1300 X 1030 format ( $6.7 \times 6.7\ \mu\text{m}^2$  pixels) charge coupled device with a fiber-optic-coupled scintillator (Photonic Sciences Ltd., “X-ray Fast Digital Imager”). The multilayer optics is a Confocal Max-Flux Optics, CMF-12-38Cu6, from Osmic Inc. A multilayer optic is an x-ray mirror that reflects only one wavelength (energy). Thus, a multilayer provides an ideal, monochromatic spectrum for imaging with a CRL. However, it is not sufficient that the radiation be monochromatic; the x-rays must also pass through the full field of view on the sample and converge toward the aperture of the CRL. The condition is met by focusing optics developed for x-ray diffraction studies. The optic was designed to deliver the maximum possible x-ray flux to a  $200\ \mu\text{m}$  spot with minimum divergence. The optic has an approximately  $1 \times 1\ \text{mm}^2$  output aperture and focuses to a spot of 38 cm away from the optic. Importantly, the local divergence at each point of the output is approximately 1 mrad, which is sufficient to fill the aperture of the CRL for each point on the object. If the divergence were too small, not enough x-rays would be collected by the lens to form an image.

Images of objects were obtained using either a microspot or an area x-ray tube source. The detector noise was subtracted out, and the source background was compensated. Thus, images were taken with the object (raw image) and

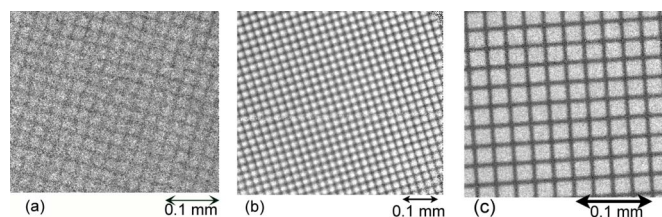


FIG. 3. Images of a 1000 mesh grid ( $6\ \mu\text{m}$  wires separated by  $19\ \mu\text{m}$ ) taken with (a) bubble lens and unfiltered area source at  $4\times$  magnification, at 250 W for 30 min; (b) bubble lens and multilayer optic at  $4\times$  magnification, at 12.5 W for 10 min; (c) parabolic lens and multilayer optic at  $10\times$  magnification, at 25 W for 10 min.

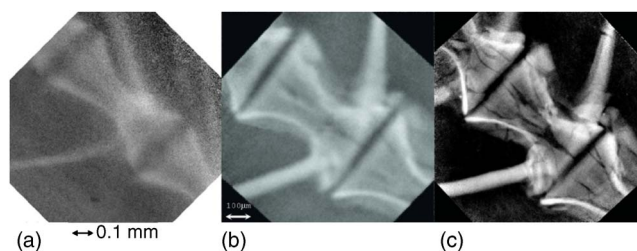


FIG. 4. Images of the spine of *Paracheirodon innesi* taken with (a) bubble lens, area source and no condenser optic at 300 W for 20 min; (b) bubble lens and multilayer condenser at 25 W for 4 h; (c) parabolic coin lens and multilayer condenser at 25 W for 10 min. The width of the vertebrae are about  $500\ \mu\text{m}$ .

without the object (source image). Also an image without source was taken to measure the detector noise (detector noise). The processed image of the object was obtained from  $(\text{raw image} - \text{detector noise}) / (\text{source image} - \text{detector noise})$ . The process would eliminate any source nonuniformity and inherent detector noise in our imaging system. The images taken of grids are presented in Fig. 3. These images give a strong qualitative presentation of the improved resolution of the imaging system. Figure 3(a) was taken with a bubble lens and an area x-ray tube, Fig. 3(b) was with a bubble lens and a microspot tube with the multilayer optics, and Fig. 3(c) is with a 92-element parabolic lens and a microspot tube and the multilayer optics. Whereas  $6\ \mu\text{m}$  wires were just resolved in the original system, with improvements to the source and CRL,  $6\ \mu\text{m}$  wires are clearly resolved and with much greater contrast. Indeed, even at 2.5 times greater magnification the contrast improved over the previous system.

One imaging task that we repeated was looking at the cartilage of a *Paracheirodon innesi*, or neon tetra aquarium fish. In Fig. 4(a), we presented an image of a spine of this fish with a bubble lens and an area x-ray tube.<sup>1</sup> Figure 4(b) is taken with a bubble lens and a microspot tube with the multilayer optics and Fig. 4(c) is with the 92-element parabolic lens and the multilayer optics. Given our improved resolution, we zoomed in to image individual vertebrae, as shown in Figs. 4(b) and 4(c). These images show clear improvement in the image quality. Note that the cracks seen in the parabolic lens image [Fig. 4(c)] may not have been in the sample at the time previous images were taken as sample had dried between experiments. We also imaged a Caribbean Grass Sponge to look at a lower contrast object with fine features and to look at the effects of contrast agents (Fig. 5). Figures 5(a)–5(c) were taken with the 92-element parabolic lens and a microspot tube with the multilayer optics. These were not tightly controlled medical experiments, but rather a preliminary qualitative examination. We looked at three con-

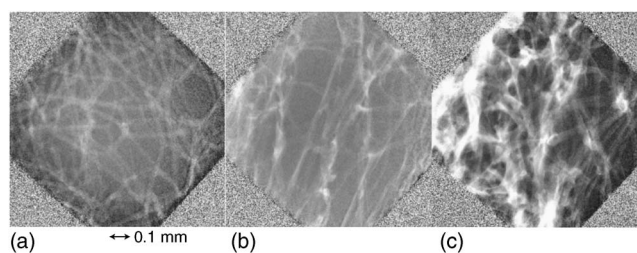


FIG. 5. Images of Caribbean Grass Sponge taken for 10 min at 25 W. Diagonal width of the FOV is 1 mm. (a) Natural sponge; (b) with 1% iodine solution; (c) with Fenesta VC contrast agent.

ditions: a natural sponge, a sponge with 1% iodine solution, and a sponge with Fenestra VC vascular contrast agent, which was provided to us a trial by its producer, Alerion Biomedical.<sup>7</sup> Both the iodine and Fenestra VC were added by soaking and then wringing the sponge to remove the liquid, leaving only a residual quantity in the sponge. While there is sufficient contrast to see the sponge without a contrast agent, the agents do increase the available signal. Interestingly, the Fenestra VC appears to thicken the strands of the sponge, which may be due to size of the molecules used in the agent, though further study would be needed to confirm this.

The resolution was estimated by drawing a line profile across the image of 25  $\mu\text{m}$  thick gold foil, taken with the 155-element parabolic lens at the magnification at 18.4. We took five line profiles from the image and added them up. The line profile of the measured knife edge response is given in Fig. 6. The resolution of one of the edges is seen to be 1.1  $\mu\text{m}$  (distance between the changes in contrast of 20%–80%). This resolution is far above the diffraction-limited resolution of  $0.61\lambda/NA=169\text{ nm}$ . The minimum resolution due to the detector pixel size can be calculated at  $M=18.4$  as  $6.7\text{ }\mu\text{m} \times 2/18.4=0.73\text{ }\mu\text{m}$ . Here we assume at least 2 pixels are needed to resolve an object. The use of parabolic lenses and some form of filtering of the source are essential to improving image resolution. Earlier we reported 6  $\mu\text{m}$

resolution with a spherical bubble lens and with an area x-ray tube source.<sup>1</sup> Resolutions better than 0.3  $\mu\text{m}$  have been achieved by others using high-quality parabolic CRLs of Al and a synchrotron source.<sup>3</sup>

This work was supported by the United States National Science Foundation under the Small Business Innovative Research Program (Grant No. DMI-0450518), by the United States Department of Health and Human Services under the Small Business Innovative Research Program (Grant No. 1 R43 RR021242-01), and by the Byelorussian Foundation of Fundamental Investigations (Grant No. F03MC-005).

<sup>1</sup>M. A. Piestrup, C. K. Gary, H. Park, J. L. Harris, J. T. Cremer, R. H. Pantell, Y. I. Dudchik, N. N. Kolchevsky, and F. F. Komarov, *Appl. Phys. Lett.* **86**, 131104 (2005).

<sup>2</sup>Y. I. Dudchik, N. N. Kolchevsky, F. F. Komarov, M. A. Piestrup, J. T. Cremer, C. K. Gary, H. Park, and A. M. Khounsary, *Rev. Sci. Instrum.* **75**, 4651 (2004).

<sup>3</sup>B. Lengeler, C. G. Schroer, M. Richwin, J. Tümmeler, M. Drakopolulos, A. Snigirev, and I. Snigireva, *Appl. Phys. Lett.* **74**, 3924 (1999).

<sup>4</sup>Y. Kohmura, K. Okada, A. Takeuchi, H. Takano, Y. Suzuki, T. Ishikawa, T. Ohigashi, and H. Yokosuka, *Nucl. Instrum. Methods Phys. Res. A* **467-468**, 881 (2001).

<sup>5</sup>A. Snigirev, V. Kohn, I. Snigireva, and B. Lengeler, *Nature (London)* **384**, 49 (1996).

<sup>6</sup>R. H. Pantell, J. Feinstein, H. R. Beguristain, M. A. Piestrup, C. K. Gary, and J. T. Cremer, *Appl. Opt.* **42**, 719 (2003).

<sup>7</sup>Alerion Biomedical Inc., San Diego, CA 92121.